DOI: 10.1002/chem.200501201

Solvent Exchange in Thermally Stable Resorcinarene Nanotubes

Heidi Mansikkamäki,[a] Sara Busi,[b] Maija Nissinen,[a] Antti Åhman,[a] and Kari Rissanen*[a]

Abstract: The assembly of *C*-methyl resorcinarene into a tubular supramolecular solid-state structure, its thermal stability, and its hosting properties are reported. Careful control of the crystallisation conditions of *C*-methyl resorcinarene and 1,4-dimethyl-1,4-diazoniabicyclo[2.2.2]octane (1,4-dimethyl DABCO) dibromide leads to a formation of two crystallographically different, but structurally very similar, solid-state nanotube structures. These structures undergo a remarkable variety of supramolecular interactions, which lead to the formation of 0.5 nm diameter nonpolar tubes through the crystal lattice. The formation of these tubes is templated by suitably sized small alcohols, namely, *n*-propanol, 2-propanol, or *n*-butanol. The self-assembly involves close π···π interactions between the adjacent resorcinarenes, and C–H···π and cation···π interactions between the resorcinarenes and the guest 1,4-dimethyl DABCO dications. The crystals of these supramolecular tube structures are thermally very stable and the included solvent alcohol can be removed from the tubes without breaking the single-crystalline structure of the assembly. After removal of the solvent molecules the tubes can be filled with other small, less polar solvent molecules such as dichloromethane.

Keywords: crystal engineering · host–guest systems · nanotubes · resorcinarenes · supramolecular chemistry

Introduction

Crystal engineering, the ability to design and prepare molecular crystal structures by using the self-assembling properties of molecular species, is emerging as a powerful strategy to develop novel, functional, nanoscale materials. When successful, this bottom-up construction of organic materials from molecules or ions through weak interactions can have a very high overall efficiency and built-in error correction compared to traditional covalent synthesis methods.[1–3] The design of supramolecular materials offers great challenges, especially when large multifunctional building blocks such as calixarenes or resorcinarenes are utilised. The design of the structures and the experiments leading to them still very much depend on trial and error and the practical experience of the chemist, rather than on the results of computational methods or models. From a material science point of view a major drawback of organic self-assembled structures is their lack of stability, since the structures are often stable only under certain, often very limited, conditions.[4–6] This is especially true for organic self-assembled nanotube structures, in which the desired functions of controlled storage, transport, and the release of suitable guests are based on weak interactions between the interior of the tube or pore and the guests.[2,7] Some exciting structures have been fabricated to address these challenges, such as the peptide nanotube crystals presented by Görbitz et al., in which the cocrystallised solvent molecules can be removed from the crystal lattice and be replaced by other small molecules.[8]

In our studies of self-assembling materials, we have used resorcinarene compounds as building blocks. Resorcinarenes and their pyrogallol analogues, pyrogallarenes (Scheme 1), possess electron-rich cavities and are commonly found in a bowl-shaped conformation, also known as the crown conformation, in which the upper rim has either eight hydroxyl groups (resorcinarenes), or in the case of pyrogallarenes, twelve hydroxyl groups.

Crystal engineering using resorcinarenes and pyrogallarenes is based on interactions of the hydrophilic upper and hydrophobic lower rim of the molecule and interactions of

[a] H. Mansikkamäki, Prof. Dr. M. Nissinen, A. Åhman, Prof. Dr. K. Rissanen
NanoScience Center, Department of Chemistry
Laboratory of Organic Chemistry, University of Jyväskylä
PO Box 35, 40014 JYU (Finland)
Fax: (+358) 14-260-2651
E-mail: Kari.Rissanen@jyu.fi

[b] S. Busi
Department of Chemistry, Laboratory of Inorganic Chemistry
University of Jyväskylä
PO Box 35, 40014 JYU (Finland)

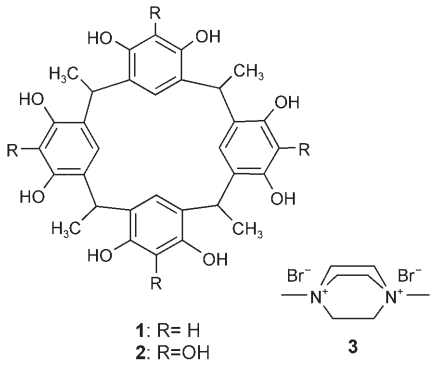

Scheme 1. The molecular structure of **1**, **2**, and **3**.

the electron-rich cavity. The upper rim hydroxyl groups form intra- and intermolecular hydrogen bonds, and the π basic cavity forms complexes with neutral molecules through C−H···π and/or π···π interactions,[9–11] and with cationic species, through cation···π interactions.[9,10,12,13] These properties have been used in, for example, complexing biologically active acethylcholine in the solid state[14] and in solution.[15] The packing of these complexes or aggregates can be further controlled by hydrophilic interactions; the longer the lower rim alkyl chains, the more probable it is that layers composed of hydrophilic and hydrophobic regions occur.[13,16]

Undoubtedly, one of the most fascinating properties of readily available resorcinarenes and pyrogallarenes is their ability to form molecular capsules. MacGillivray and Atwood[17] were the first to discover that resorcinarenes can form a hexameric, solvent-mediated capsular assembly of *C*-methyl resorcinarene (**1**) that can now, eight years later, be considered as an icon for self-assembled molecular capsules. The hexameric structure of **1** is found in virtually every modern textbook of supramolecular chemistry. A few years later Mattay and co-workers[18] reported the crystal structure of a directly hydrogen-bonded hexameric capsule of tetraisobutyl pyrogallarene. Aoki and co-workers and Atwood and co-workers reported almost simultaneously the structures of solvent-mediated dimeric capsules of alkyl resorcinarenes encapsulating tetraethyl ammonium cations or solvent molecules, respectively.[19,20] These findings have been followed by several studies on dimeric[6,13,21] and hexameric[22] capsules of unsubstituted resorcinarenes and pyrogallarenes in the solid state, in solution, or in the gas phase. To date all the resorcinarene capsules fabricated have been solvent mediated; however, the four additional hydroxyl groups in pyrogallarenes makes it possible for them to directly hydrogen bond to each other forming either hexameric[18] or dimeric[23] capsules.

During the course of our encapsulation studies of diquaternary alkyl ammonium cations by *C*-methyl resorcinarene (**1**) the crystals of a novel tubular solid-state structure of **1** with 1,4-dimethyl-1,4-diazoniabicyclo[2.2.2]octane (1,4-dimethyl DABCO) dibromide (**3**) were successfully isolated.[24] The tube structure is held together by multiple offset face-to-face π···π interactions in between the neighbouring molecules of **1** that further pack to form the backbone of a nanotubular structure (Figure 1). The lower rim methyl groups of **1** are found in the interior of the hydrophobic tube, while each of the hydroxyl groups and cavities of **1** that complex a diquaternary cation of **3** are on the outer surface, making the surface hydrophilic.[24]

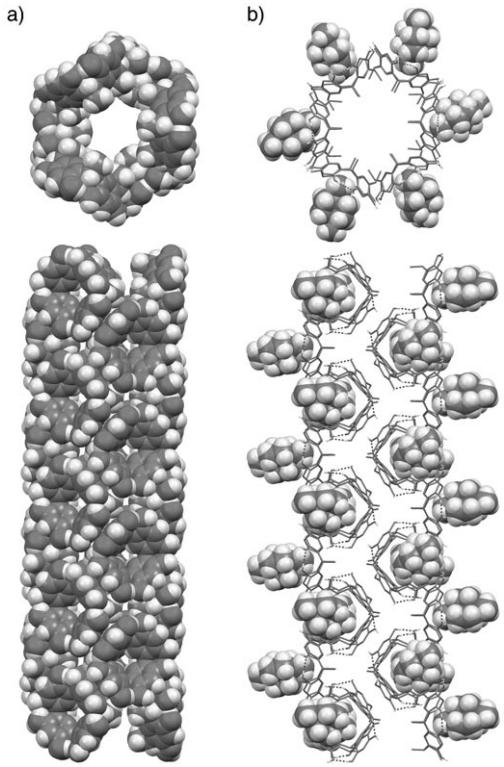

Figure 1. Two different views of the crystal structure of the resorcinarene nanotube, along the tube and perpendicular to it. a) A CPK presentation (the salt **3** and the cocrystallised solvents are omitted for clarity). b) The tube skeleton in stick presentation with the cations in CPK style (hydrogen atoms of **1**, disordered cations, anions, and water molecules are omitted for clarity).

The resorcinarene tube structure is unique among the large variety of resorcinarene assemblies in existence. Also, for the closely related calixarenes only a few examples of calixarene nanotubes, namely, tubular structures constructed of *p*-sulfonatocalix[4]arene[25] and calixhydroquinone,[26] are known. In both of these the packing of the calixarenes differs considerably from the packing of the *C*-methyl resorcinarenes shown in Figure 1.

Herein we describe crystal-engineering studies, namely the effect of the solvent and the host on the formation of the solid-state nanotube by means of single-crystal X-ray diffraction studies, and thermal stability studies of the tube crystals, by means of thermogravimetric/differential thermal analysis (TG/DTA), differential scanning calorimetry (DSC) and X-ray powder diffraction techniques. Results detailing the removal of solvent alcohols and their substitution by other organic solvent molecules are also presented.

Results and Discussion

In our previous studies of resorcinarene capsules and open complexes, molecules of the crystallization solvents cocrystallised without exception.[6,13] This resulted in thermally unstable crystals, which decomposed in most cases when taken out of the mother liquor. After the discovery of the triclinic resorcinarene nanotube structure $\mathbf{T_{tric}}$ (Figure 1) with a composition of $3\,C_{32}H_{32}O_8{\cdot}4\,C_8H_{18}N_2Br_2{\cdot}6\,H_2O$($\mathbf{1}_3{\cdot}\mathbf{3}_4{\cdot}6\,H_2O$), we noticed that the tube crystals were surprisingly stable in air at room temperature (RT), relative to the crystals of the dimeric capsules of **1** and diprotonated DABCO dichloride or 1,4-dimethyl DABCO dibromide.[13a] These capsule crystals decomposed within an hour upon exposure to air owing to the evaporation of weakly bound cocrystallised solvents.

Inspired by this observation, several batches of tube crystals were prepared for detailed thermal-stability measurements. During the crystallization experiments it was noticed that, in addition to needlelike crystals of $\mathbf{T_{tric}}$, single crystals of a different morphology were also obtained under the same conditions (Figure 2).

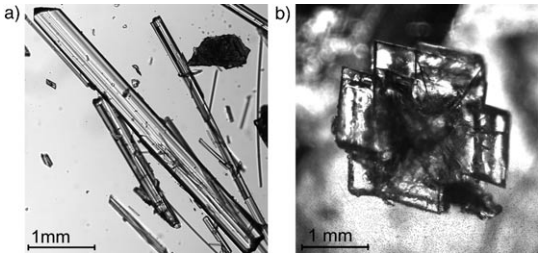

Figure 2. Light-microscope images of the two differently shaped crystals. a) Needlelike tube crystals of $\mathbf{T_{tric}}$ and b) flowerlike aggregates of plate-shaped crystals.

The crystal structure of these platelike crystals reveals a nontubular, open 1:1 complex (**OR**) with a composition of $C_{32}H_{32}O_8{\cdot}C_8H_{18}N_2Br_2{\cdot}3\,H_2O$ (**1**·**3**·$3\,H_2O$). As expected, the cations are positioned inside the resorcinarene bowls (Figure 3), now in a horizontal position, whereas in $\mathbf{T_{tric}}$ the cations complexed in the resorcinarenes are in a vertical position with one of the methyl groups pointing into the resorcinarene cavity. In **OR** there are also three water molecules per asymmetric unit; two of them are hydrogen bonded to the resorcinol hydroxyl groups and one is positioned between the lower rim methyl groups of **1**.

Changing the ratios of **1** and **3** or the concentrations of the *n*-propanol (aqueous) solutes in the crystallization experiments did not have an effect on the crystallized $\mathbf{T_{tric}}$/**OR** ratio; crystals of both structures were found in each experiment. In previous studies we found that the conditions leading to the formation of $\mathbf{T_{tric}}$ were very sensitive to the influence of the anion. Attempts to crystallize similar tubular architectures from **1** and a corresponding 1,4-dimethyl DABCO dichloride or diiodide instead of the bromide salt **3**, led only to the formation of an open nontubular 1:1 complex with the dichloride salt.[24] To elucidate the effect of the host structure on the tube-structure formation, resorcinarene **1** was substituted with pyrogallarene **2**; it was hypothesized that **2** might form a similar tubular structure when crystallized under the same conditions as the resorcinarene tube. From a solution of the sample in *n*-propanol, measurable crystals of a complex of **2** with **3** resulted within one day. This nontubular open complex, **OP**, has the composition $C_{32}H_{32}O_{12}{\cdot}1.5\,C_8H_{18}N_2Br_2{\cdot}C_3H_8O$ (**2**·$\mathbf{3}_{1.5}$·*n*-propanol). The structure of this open complex is clearly different from the resorcinarene complex **OR**. In **OP** two of the three cations are complexed by pyrogallarenes and the uncomplexed, disordered and more weakly bound cation is positioned in the same layer as the ordered cations and anions (Figure 4).

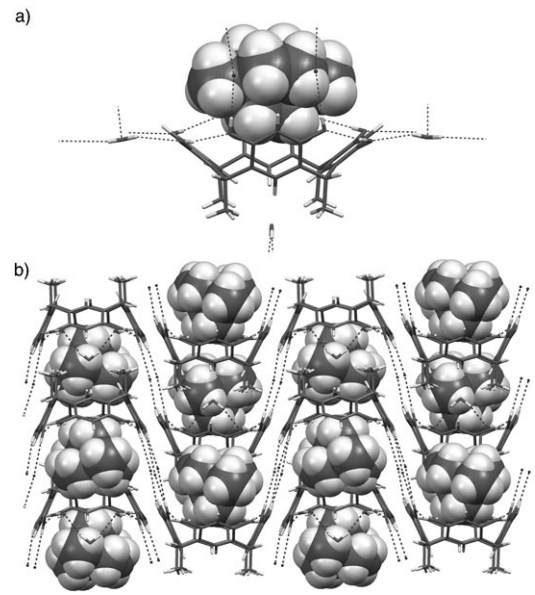

Figure 3. The crystal structure of the nontubular complex, **OR**: a) the asymmetric unit and b) the packing mode along the crystallographic *c* axis. The cations are shown in CPK style; the resorcinarenes, anions, and cocrystallised water molecules are shown in stick presentation. Hydrogen bonds are shown with dashed lines.

The anions are hydrogen bonded between two pyrogallarene molecules with cocrystallised *n*-propanol molecules. The

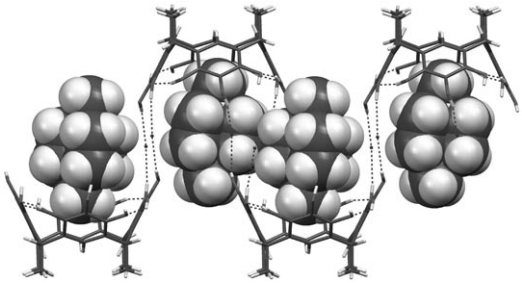

Figure 4. Packing of **OP**: molecules of **2** and the Br^- ions are shown in stick presentation and the cations of **3** are drawn in CPK style. The disordered cations and *n*-propanol solvent molecules are omitted for clarity. Hydrogen bonds are shown with dashed lines.

pyrogallarenes form a hydrophobic layer, while the salts and solvent molecules form a hydrophilic one. These results confirm that the formation of the nanotube structure is unique for the complex formed by **1** and **3**; any change in either the host structure (one additional hydroxyl group in the 2-position), the anions (chloride instead of bromide) or the cations (diprotonated DABCO or dibenzyl DABCO instead of dimethyl DABCO), hinders the tube formation, resulting in various open 1:1 structures or other structures.

No tubes were formed without the combination of resorcinarene **1** and **3**. However, in the course of the recrystallisation studies it was found that tubular $\mathbf{T}_{tric}$ also crystallises from aqueous *n*-butanol and 2-propanol, in addition to *n*-propanol. Surprisingly, when toluene was diffused into the solvent alcohol to enhance the efficiency and speed of the crystallization, a new tube structure $\mathbf{T}_{trig}$ was obtained from the same alcohols. This structure is essentially the same as $\mathbf{T}_{tric}$, when the resorcinarenes and the tube structures are considered. The composition of $\mathbf{T}_{trig}$ is $3\,C_{32}H_{32}O_8{\cdot}4\,C_8H_{18}N_2Br_2{\cdot}8\,H_2O$ ($\mathbf{1}_3{\cdot}\mathbf{3}_4{\cdot}8\,H_2O$), the only difference being the amount of cocrystallised water, which is two molecules more in $\mathbf{T}_{trig}$. The $\mathbf{T}_{trig}$ structure (Figure 5a) with a trigonal lattice symmetry and space group $P\bar{3}$ is more ordered than the previously reported triclinic tube structure $\mathbf{T}_{tric}$ with space group $P\bar{1}$. Whereas many of the anions and water molecules are severely disordered in $\mathbf{T}_{tric}$, they are well ordered in $\mathbf{T}_{trig}$. The positions of the cations in $\mathbf{T}_{trig}$ are the same as in $\mathbf{T}_{tric}$ and three of the four cations are present in an upright position in the resorcinarene cavities, allowing close C–H···π and cation···π interactions with **1**. The fourth cation, which is equally disordered over two positions, merely completes the salt layer and fills the interstices in the crystal lattice. The Br^- ions are hydrogen bonded to the hydroxyl groups of **1** and interact with the cations by electrostatic forces. A view of the packing of $\mathbf{T}_{trig}$ along the chrystallographic *c* axis is presented in Figure 5a. The tube interior of $\mathbf{T}_{trig}$ is shaped like a line of stacked hourglasses, the shortest van der Waals diameter is 0.5 nm. The van der Waals volume, that is, the solvent accessible volume of the tube interiors, takes up approximately 10% of the total-crystal volume. In $\mathbf{T}_{tric}$ and also in the case of $\mathbf{T}_{trig}$ a significant amount of electron density (1.4–1.0 e $Å^{-3}$) was found inside the tube that could not, due to severe disorder, be assigned to a chemically reasonable model. The presence of the crystallization solvents (2-propanol and toluene used in the diffusion experiment) could not therefore be verified; however, thermal analysis (see below) supported the view that the residual electron density found inside the tubes in $\mathbf{T}_{tric}$ and $\mathbf{T}_{trig}$ was indeed *n*-propanol. The altered recrystallisation conditions, namely toluene diffusion into the alcohol, changed the morphology of the crystals from thin needles to large blocks, at the same time inhibiting the formation of the open 1:1 complex **OR**.

The observed stability under ambient conditions urged us to study the thermal stability of the tube crystals. The needlelike crystals of $\mathbf{T}_{tric}$ were manually separated from the platelike crystals of **OR** under a light microscope. TG/DTA

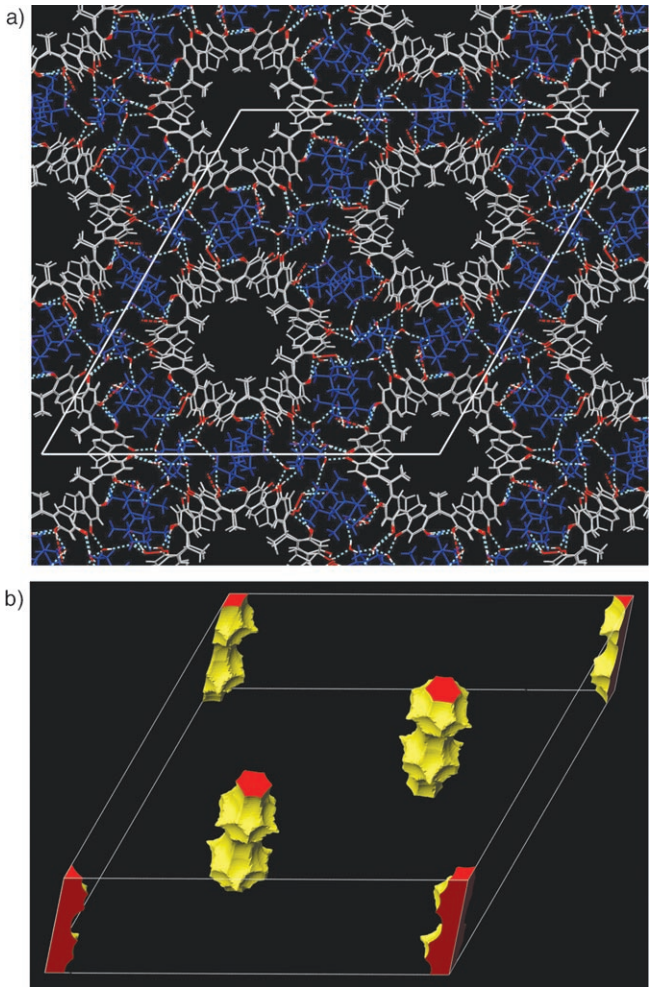

Figure 5. a) Packing of $\mathbf{T}_{trig}$ along the crystallographic *c* axis. The cations of the salts are highlighted in blue and the hydrocarbon skeletons of **1** in grey. Hydrogen bonds are shown with dashed lines. b) Solvent accessible voids (the size of a water molecule) in one unit cell are shown with yellow surfaces and the unit cell cut-offs along or parallel to the tubes are shown in red.

and DSC measurements were performed on both complexes and separately on the starting materials **1** and **3**. The TG/DTA curves of compounds **1**, **3**, $\mathbf{T}_{tric}$, and **OR**, are presented in Figure 6. The thermal decomposition of resorcinarene **1** started at 327 °C (Figure 6), while the DABCO salt **3** started to decompose at 259 °C (Figure 6b). Crystals of both $\mathbf{T}_{tric}$ and **OR** were taken out of the crystallization liquid and left to dry in air for approximately one hour before the TG/DTA measurements. In the case of $\mathbf{T}_{tric}$ (Figure 6c), a slight decrease can be seen in the beginning of the TG mass-loss curve, indicating that some solvents are continuously being evaporated. In the range 70–90 °C there is a small drop in the TG curve; this drop is due to weakly bound *n*-propanol solvent molecules evaporating from the tube interior. On the basis of the DTA curves, no indication of melting or solid–solid phase transitions can be seen for $\mathbf{T}_{tric}$ below 252 °C in which, as mentioned before, the DABCO salt **3** starts to decompose. This behaviour was also confirmed by

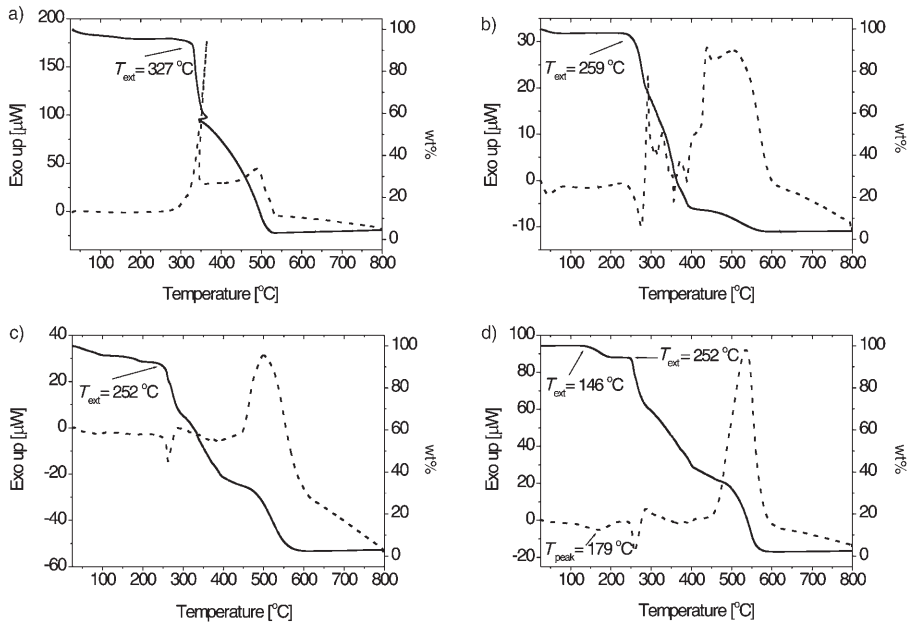

Figure 6. The TG (solid line) and DTA curves (dashed line) of a) **1**, b) **3**, c) $\mathbf{T_{tric}}$ and d) **OR**.

DSC measurements and on the basis of these results, repeated with three different samples, the tube structure remained intact up to the point at which decomposition of **3** began. The open complex **OR** showed different thermal behaviour. While the beginning of the TG curve (Figure 6d) is straight, a drop and hence a loss of the cocrystallised water molecules starts after 140 °C and is complete at 180 °C.

This weight loss corresponds exactly to the loss of three water molecules per resorcinarene. On the basis of DTA and DSC measurements we can conclude that the original supramolecular structure was lost during the evaporation of water. To verify similar behaviour also observed for the trigonal tube, TG/DTA measurements were performed on block crystals of $\mathbf{T_{trig}}$. As expected, the stability results obtained for $\mathbf{T_{trig}}$ and $\mathbf{T_{tric}}$ were similar.

To further confirm the single-crystal stability of the tube structure and the ability of the crystals to survive intact in temperatures above the boiling points of the crystallization solvents, crystals of $\mathbf{T_{tric}}$ and $\mathbf{T_{trig}}$ were placed in an oven at 100 °C for one hour. After this time the powder diffraction patterns were measured and compared with patterns of unheated crystals. All of these diffraction patterns were then compared to the theoretical diffraction patterns calculated from the unit-cell parameters of $\mathbf{T_{tric}}$ and $\mathbf{T_{trig}}$.

In the case of $\mathbf{T_{tric}}$ the calculated and experimental diffraction patterns did not agree very well, as the experimental powder diffraction sample of $\mathbf{T_{tric}}$ was contaminated with crystals of the cocrystallised **OR**. Several crystallization and separation attempts gave the same results, indicating that manual separation of the $\mathbf{T_{tric}}$ and **OR** crystals in sufficient amounts for powder diffraction measurements was not possible. However, the high-intensity peaks of $\mathbf{T_{tric}}$ (in the 2θ range $<5°$) could be seen in the experimental powder diffraction patterns (of both the heated and unheated samples). However, the high-angle part of the powder diffraction pattern remained ambiguous, because the low-intensity peaks of $\mathbf{T_{tric}}$ were much weaker and less distinctive than the high-intensity peaks measured at low angles. Minute amounts of the contaminant complex **OR** made interpretation of the pattern difficult, so that only ambiguous results of the thermal stability of $\mathbf{T_{tric}}$ crystals were obtained from powder diffraction methods. However, the well-ordered and contaminant-free $\mathbf{T_{trig}}$ gave encouraging results (Figure 7).

The experimental diffraction pattern of $\mathbf{T_{trig}}$ agrees well with the calculated pattern owing to the fact that large block crystals of $\mathbf{T_{trig}}$ were readily available. The calculated diffraction pattern of $\mathbf{T_{trig}}$ fits very well to the

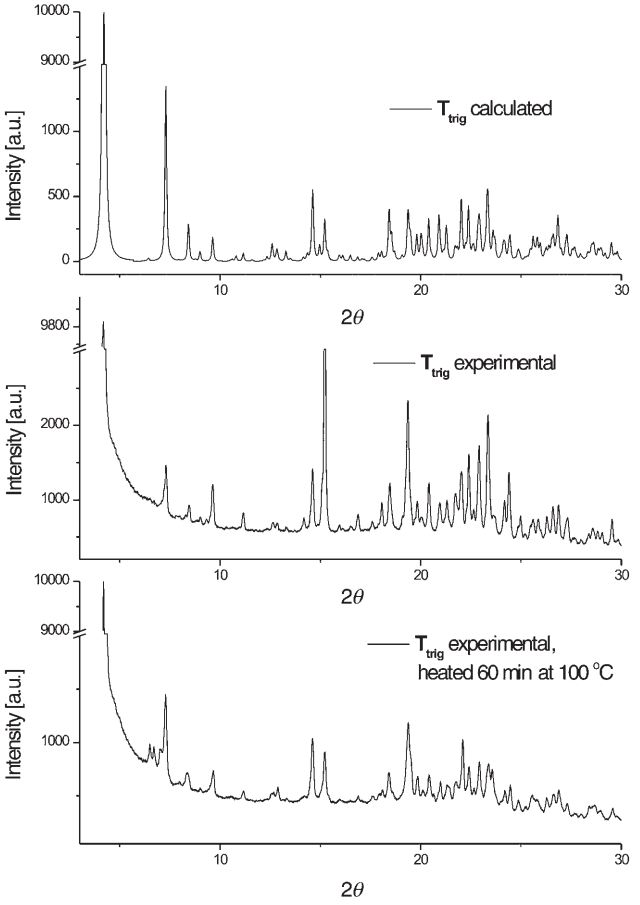

Figure 7. Results of calculated and experimental powder diffraction analysis of $\mathbf{T_{trig}}$.

experimental pattern measured from crystals heated at 100 °C for an hour. Based on the TG/DSC and powder diffraction results it can be concluded that the tube structure $\mathbf{T_{trig}}$ is very stable at least up to 100 °C.

The stability of the tube crystals and the nonpolar interior of the 0.5 nm tubes led us to look for possible functionalities or applications of these intriguing structures. To explore the storage capability for small molecules we heated the crystals of $\mathbf{T_{tric}}$ at 100 °C for half an hour to remove the cocrystallised disordered solvent molecules from the tube interior, as shown by the TG studies. After heat treatment the crystals were soaked in acetonitrile, chloroform, dichloromethane, dibromomethane (DCM), benzene and toluene. Water could not be used since the crystals decomposed in water. The X-ray structure of one of the heated crystals was measured directly after heating. The single-crystal nature of the crystals was retained with only a slight loss of crystal quality; the structure showed considerably lower electron density inside the tube (electron density not higher than 1 e $Å^{-3}$) than that which was observed for a nonheated $\mathbf{T_{tric}}$ tube. Crystal structures of the soaked crystals were measured after keeping them for two to four weeks in the corresponding solvent. All of the crystal structures determined for soaked $\mathbf{T_{tric}}$ crystals showed clear differences in the residual electron density, which in each case was concentrated in the tube interior, indicating the presence of disordered solvents. In one case only, namely the crystal soaked in DCM, was the assignment of the solvent inside the tube unambiguous. A DCM molecule with an occupation factor of 0.5 was determined per asymmetric unit. The composition of this tube structure, $\mathbf{T_{tric}DCM}$ is $3\,C_{32}H_{32}O_8{\cdot}4\,C_8H_{18}N_2Br_2{\cdot}6\,H_2O{\cdot}0.5\,CH_2Cl_2$ ($\mathbf{1}_3{\cdot}\mathbf{3}_4{\cdot}6\,H_2O\cdot 0.5\,$DCM). However, in this structure some residual electron density inside the tube interior could not be assigned to a chemically meaningful model either. This means that in addition to the disordered DCM molecules (assigned with a population parameter of 0.5), there are also other more severely disordered solvents present. The X-ray structure of $\mathbf{T_{tric}DCM}$ and the orientation of the DCM molecules inside the tube are presented in Figure 8.

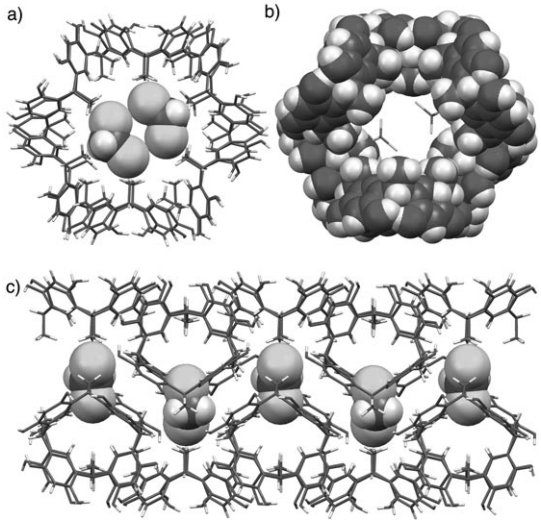

Figure 8. The X-ray structure of $\mathbf{T_{tric}DCM}$. a) A view along the tube showing all of the DMCs in disordered positions (with occupancy of 0.5), shown in CPK style; molecules of **1** are shown in stick presentation. b) A stick presentation of $\mathbf{T_{tric}DCM}$ in CPK style. c) A view perpendicular of the tube.

Conclusion

Depending on the crystallization conditions, the crystallization of **1** with **3** from a solution of aqueous alcohols can be driven to self-assemble into two different crystal structures of resorcinarene nanotubes, in which the tubes are separated by a layer of cocrystallised salt **3** and water molecules.

It is worth noting that the crystallization process of the tube structures is very subtle and any change either in the cation, anion or the host results in other types of structures. In the light of our investigations, the formation of the tubular resorcinarene structures occurs only in the presence of *n*-propanol, 2-propanol or *n*-butanol. We conclude that these small organic solvents strongly affect the initial stages of molecular association and act as templating agents for the assembly of resorcinarenes forming the supramolecular tubes. It is difficult to determine which of the various weak interactions is the driving force in the tube formation process, but undoubtedly the π–π stacking, the cation···π and C−H···π interactions between the resorcinarenes and the cations and the electrostatic interactions between the ionic groups of **3**, play important roles.

The tube crystals exhibit high stability for an organic porous supramolecular material. This is manifested by the fact that the cocrystallised solvents can be removed by using moderately high temperatures, while the tube structure itself remains intact. TG and DSC measurements indicate that the tube structures are stable up to 250 °C. This remarkable stability can be explained by the multiple weak interactions and the efficient packing of the tube skeleton and salt layers in between the tubes, that is, the salt and water layers act as cement between the self-assembled "brick" resorcinarenes.

The stability of the resorcinarene nanotube crystals and the discovery that small organic solvents can be directed in and out of the tubes without destroying the tube structure are encouraging and exciting results. These results will increase our knowledge about self-assembling tubular or porous materials and emphasise the use of supramolecular chemistry tools to develop new solutions and strategies for storage, removal or transport of volatile small organic molecules or gases.

Experimental Section

Crystals of **OR** were obtained by slow evaporation from a 2:1 mixture of compound **1** (54.5 mg) and salt **3** (15.1 mg) dissolved in aqueous *n*-propanol (ca. 4 mL; two drops of water). These are the same conditions and reaction mixture from which the previously reported tube, $\mathbf{T_{tric}}$, was crystallized. $\mathbf{T_{trig}}$ was crystallized from an aqueous *n*-propanol solution (ca. 4 mL) of **1/3** in the ratio 3:4 (81.5 mg of **1** and 60.5 g of **3**) by slow diffu-

sion of toluene. The same structure was also obtained by slow diffusion of toluene into solutions of different ratios of **1** and **3** in either aqueous 2-propanol or *n*-butanol. **T_{tric}DCM** crystals were obtained by gently warming crystals of **T_{tric}** at 100 °C for 30 min and then placing the intact crystals in DCM for two weeks, after which time the single-crystal structure was measured. Crystals of **OP** were obtained from an aqueous *n*-propanol solution (ca. 4 mL) of **2**/**3** in the ratio 3:4 (91.2 mg of **2** and 60.5 mg of **3**) by slow evaporation.

Single-crystal X-ray structures: The single-crystal X-ray crystallographic data for all structures were recorded with a Nonius Kappa CCD diffractometer. Graphite monochromatised $Mo_{K\alpha}$ radiation ($\lambda = 0.71073$ Å) and a temperature of 173.0 ± 0.1 K were used in all cases. The CCD data were processed with Denzo-SMN v0.95.373.[27a] All structures were solved by direct methods (SHELXS-97)[27b] and refined against F^2 by full-matrix least-squares techniques (SHELXL-97)[27c] by using anisotropic thermal displacement parameters for all non-hydrogen atoms of **1**, anions, ordered cations, and solvent molecules. All of the OH hydrogen atoms could be found from the difference Fourier map of **OR** and **T_{trig}** and some of them could be found from **T_{tric}DCM**, while the rest of the OH hydrogen atoms and all of the C hydrogen atoms were calculated at their idealised positions with isotropic temperature factors (1.2 or 1.5 times the C temperature factor) and refined as riding atoms. The hydrogen atoms of most of the water molecules were not determined. In the structures **T_{trig}**, **T_{tric}DCM** and **OP** the severely disordered cation, anion and solvent molecules were refined isotropically. In the case of **OR** and **OP** an empirical absorption correction was applied,[27d] while in the structures **T_{trig}** and **T_{tric}DCM** an absorption correction was performed but was not applied in the final refinement, since no improvement was detected in the data. In the tubular structure **T_{trig}** notable electron density was found in the interior (from 1.4 to 1.0 e Å^{-3}), but could not be assigned to a chemically reasonable model of, for example, solvent molecules. An electron density of 4.0 e Å^{-3} was found between a bromide anion and the aqueous solvent (1.25 Å from O87 and 2.10 Å from Br8) and an electron density of 1.1 e Å^{-3} was found 1.0 Å away from Br7. These are artefacts resulting from either the large size or quality of the crystal. In the tube structure **T_{tric}DCM** some residual electron density was found (maximum of 4.0 e Å^{-3}) inside the tube and left unassigned, in addition to the disordered DCM molecule with a population parameter of 0.5. The largest peak found in between the methyl groups of one of the resorcinarenes was at a distance of 4.1 Å from the methyl carbon atoms. In the structure **OP** some residual electron density that could be assigned to severely disordered *n*-propanol molecules was removed by using the program SQUEEZE.[27e] The crystal data are presented in Table 1. CCDC 282422-282425 contain the supplementary crystallographic data for this paper. These data can be obtained free of charge from The Cambridge Crystallographic Data Centre via www.ccdc.cam.ac.uk/data_request.cif.

X-ray powder diffraction analyses: The powder diffraction data of the crystals were measured to confirm the structural similarities between all crystals formed and also to prove the thermal stability of the crystals. The calculated powder diffraction data were obtained from the structural parameters of each of the compounds by using the Mercury software package.[28] X-ray powder diffraction data were obtained at room temperature by a Huber G670 imaging-plate Guinier camera. The sealed-tube X-ray generator system was operated at 45 kV and 25 mA, and pure line-focused $Cu_{K\alpha 1}$ radiation ($\lambda = 1.5406$ Å) was produced by using a primary-beam-curved germanium monochromator ($d = 3.266$ Å). The measurements were carried out with a Guinier-type transmission geometry by using an angle of incidence of 45° to the sample normal. The diffracted X-ray photons with an angular range of 4–100° (2θ) were captured on a curved imaging-plate detector and the diffraction data were recorded with a step resolution of 0.005 (2θ).

Thermal studies: The thermal decomposition paths of the starting materials, **1** and **3**, and the decomposition paths of the supramolecular complexes of these materials, namely crystals of **T_{trig}** and **OR** were determined. The data were obtained with a Perkin–Elmer Diamond TG/DTA instrument. The measurements were carried out by using platinum pans under a synthetic air atmosphere (flow rate 110 mL min^{-1}). The sample weights used in the measurements were in the range 2–10 mg.

The DSC measurements were performed with a Perkin–Elmer PYRIS 1 DSC instrument and were carried out (under a nitrogen atmosphere at a flow rate of 50 mL min^{-1}) by using 50 μL sealed aluminium sample pans with pinholes. The temperature calibration was carried out by using three standard materials (*n*-decane, In and Zn) and the energy calibration by using an indium standard. The samples were heated at a rate of 10 °C min^{-1} from −50 °C to temperatures near the predetermined (TG/DTA) decomposition temperature of each compound. The sample weights used in the measurements were in the range 2–6 mg.

Acknowledgements

Dr. Minna Luostarinen and Dr. Christoph Schalley are thanked for providing compounds **1** and **3**, respectively. Jonna Nykky is thanked for photographing the crystals and Dr. Manu Lahtinen for practical advice on

Table 1. Crystal data and parameters (for **T_{tric}**, see reference [24]).

Structure	**T_{tric}**	**OR**	**OP**	**T_{trig}**	**T_{tric}DCM**
formula	$3\,C_{32}H_{32}O_8{\cdot}4\,C_8H_{18}$ $N_2Br_2{\cdot}6\,H_2O$	$C_{32}H_{32}O_8{\cdot}C_8H_{18}$ $N_2Br_2{\cdot}3\,H_2O$	$1\,C_{32}H_{32}O_{12}{\cdot}1.5\,C_8H_{18}$ $N_2Br_2{\cdot}C_3H_8O$	$3\,C_{32}H_{32}O_8{\cdot}4\,C_8H_{18}$ $N_2Br_2{\cdot}8\,H_2O$	$3\,C_{32}H_{32}O_8{\cdot}4\,C_8H_{18}$ $N_2Br_2{\cdot}6\,H_2O{\cdot}0.5\,CH_2Cl_2$
a [Å]	13.9358(2)	13.3503(4)	13.220(1)	41.9357(5)	14.004(3)
b [Å]	23.6272(2)	18.0960(5)	13.777(1)	41.9357(5)	23.541(5)
c [Å]	23.9065(3)	31.4469(6)	18.919(2)	14.0434(2)	23.840(5)
α [°]	64.617(1)	90	71.441(3)	90	64.42(3)
β[°]	85.811(1)	90	74.254(4)	90	85.74(3)
γ[°]	87.348(1)	90	62.159(5)	120	87.20(3)
V [Å^3]	7091.7(2)	7597.2(3)	2857.3(4)	21388.0(5)	7068(2)
Z	2	8	2	6	2
crystal system	triclinic	orthorhombic	triclinic	trigonal	triclinic
space group	$P\bar{1}$	*Pbca*	$P\bar{1}$	$P\bar{3}$	$P\bar{3}$
ρ_{calcd} [Mg m^{-3}]	1.382	1.575	1.304	1.391	1.406
crystal size [mm^{-1}]	$0.30 \times 0.30 \times 0.10$	$0.32 \times 0.27 \times 0.07$	$0.45 \times 0.45 \times 0.2$	$0.90 \times 0.80 \times 0.75$	$0.40 \times 0.20 \times 0.15$
μ [mm^{-1}]	2.33	2.20	2.17	2.32	2.36
reflections measured/unique	85764/10857	47482/3836	31089/7649	90477/14694	44202/9828
R_{int}	0.121	0.1457	0.056	0.0712	0.154
R/R_w[a]	0.090/0.227	0.056/0.094	0.064/0.150	0.059/0.155	0.112/0.285
parameters	1680	536	610	1697	1580
GOOF	1.034	1.015	1.074	1.126	1.036

[a] $I > 2\sigma(I)$.

powder diffraction measurements. H.M. thanks The Graduate School of Bio-organic and Medicinal Chemistry, and K.R., S.B., M.N., and A.Å. thank the Academy of Finland (K.R./S.B. project no. 205714 and M.N./A.Å. project no. 211240) for financial support.

[1] G. R. Desiraju, *Angew. Chem.* **1995**, *107*, 2541–2558; *Angew. Chem. Int. Ed. Engl.* **1995**, *34*, 2311–2327.
[2] D. T. Bong, T. D. Clark, J. R. Granja, M. R. Ghadiri, *Angew. Chem.* **2001**, *113*, 1016–1041; *Angew. Chem. Int. Ed.* **2001**, *40*, 988–1011, and references therein.
[3] D. Braga, L. Brammer, N. R. Champness, *CrystEngComm* **2005**, *7*, 1–19.
[4] G. R. Desiraju, *J. Mol. Struct.* **2003**, *656*, 5–15.
[5] E. Utzig, O. Pietraszkiewicz, M. Pietraszkiewicz, *J. Therm. Anal. Calorim.* **2004**, *78*, 973–980.
[6] H. Mansikkamäki, M. Nissinen, K. Rissanen, *CrystEngComm* **2005**, *7*, 519–526.
[7] a) C. H. Görbitz, *Acta Crystallogr. Sect. B* **2002**, *58*, 849–854; b) C. H. Görbitz, *New J. Chem.* **2003**, *27*, 1789–1793.
[8] C. H. Görbitz, M. Nielsen, J. Szeto, L. W. Tangen, *Chem. Commun.* **2005**, 4288–4290.
[9] a) T. Lippmann, H. Wilde, M. Pink, A. Schäfer, M. Hesse, G. Mann, *Angew. Chem.* **1993**, *105*, 1258–1260; *Angew. Chem. Int. Ed. Engl.* **1993**, *32*, 1195–1197; b) W. Iwanek, R. Frohlich, M. Urbaniak, C. Nather, J. Mattay, *Tetrahedron* **1998**, *54*, 14031–14040; c) W. Iwanek, M. Urbaniak, *Tetrahedron* **2001**, *57*, 10377–10382; d) M. Nissinen, E. Wegelius, D. Falabu, K. Rissanen, *CrystEngComm* **2000**, 151–153.
[10] M. Nissinen, K. Rissanen, *Supramol. Chem.* **2003**, *15*, 581–590.
[11] J. L. Atwood, A. Szumna, *J. Supramol. Chem.* **2003**, *2*, 479–482.
[12] I. Georgiev, E. Bosch, C. L. Barnes, M. Draganjac, *Cryst. Growth Des.* **2004**, *4*, 235–239.
[13] a) H. Mansikkamäki, M. Nissinen, K. Rissanen, *Chem. Commun.* **2002**, 1902–1903; b) H. Mansikkamäki, M. Nissinen, C. A. Schalley, K. Rissanen, *New J. Chem.* **2003**, *27*, 88–97.
[14] K. Murayama, K. Aoki, *Chem. Commun.* **1997**, 119–120.
[15] M. Demura, T. Yoshida, T. Hirokawa, Y. Kumaki, T. Aizawa, K. Nitta, I. Bitter, K. Toth, *Bioorg. Med. Chem. Lett.* **2005**, *15*, 1367–1370.
[16] a) T. Borowiak, M. Maczynski, M. Pietraszkiewicz, O. Pietraszkiewicz, *J. Inclusion Phenom. Macrocyclic Chem.* **1999**, *35*, 131–138; b) B. Ma, H. Sun, S. Gao, *Angew. Chem.* **1994**, *116*, 1398–1400; *Angew. Chem. Int. Ed.* **2004**, *43*, 1374–1376; c) Y. Tanaka, M. Miyachi, Y. Kobuke, *Angew. Chem.* **1999**, *111*, 565–567; *Angew. Chem. Int. Ed.* **1999**, *38*, 504–506.
[17] L. R. Macgillivray, J. L. Atwood, *Nature* **1997**, *389*, 469–472.
[18] T. Gerkensmeier, W. Iwanek, C. Agena, R. Frohlich, S. Kotila, C. Nather, J. Mattay, *Eur. J. Org. Chem.* **1999**, 2257–2262.
[19] K. Murayama, K. Aoki, *Chem. Commun.* **1998**, 607–608.
[20] K. N. Rose, L. J. Barbour, G. W. Orr, J. L. Atwood, *Chem. Commun.* **1998**, 407–408.
[21] a) A. Shivanyuk, K. Rissanen, E. Kolehmainen, *Chem. Commun.* **2000**, 1107–1108; b) M. Mäkinen, P. Vainiotalo, M. Nissinen, K. Rissanen, *J. Am. Soc. Mass Spectrom.* **2003**, *14*, 143–151; c) A. Shivanyuk, J. C. Friese, S. Doering, J. Rebek Jr., *J. Org. Chem.* **2003**, *68*, 6489–6496.
[22] a) A. Shivanyuk, J. Rebek Jr., *Proc. Natl. Acad. Sci. USA* **2001**, *98*, 7662–7665; b) L. C. Palmer, J. Rebek Jr., *Org. Lett.* **2005**, *7*, 787–789; c) J. Antesberger, G. W. V. Cave, M. C. Ferrarelli, M. W. Heaven, C. L. Raston, J. L. Atwood, *Chem. Commun.* **2005**, 892–894.
[23] M. Luostarinen, A. Åhman, M. Nissinen, K. Rissanen, *Supramol. Chem.* **2004**, *16*, 505–512.
[24] H. Mansikkamäki, M. Nissinen, K. Rissanen, *Angew. Chem.* **2004**, *116*, 1263–1266; *Angew. Chem. Int. Ed.* **2004**, *43*, 1243–1246.
[25] G. W. Orr, L. J. Barbour, J. L. Atwood, *Science* **1999**, *285*, 1049–1052.
[26] a) B. H. Hong, S. C. Bae, C. W. Lee, S. Jeong, K. S. Kim, *Science* **2001**, *294*, 348–351; b) B. H. Hong, J. Y. Lee, C. W. Lee, J. C. Kim, S. C. Bae, K. S. Kim, *J. Am. Chem. Soc.* **2001**, *123*, 10748–10749.
[27] a) Z. Otwinowski, W. Minor, *Methods Enzymol.* **1997**, *276*, 307–326; b) G. M. Sheldrick, *Acta Crystallogr. Sect. A* **1990**, *46*, 467–473; c) G. M. Sheldrick, T. R. Schneider, *Methods Enzymol.* **1997**, *277*, 319–343; d) R. H. Blessing, *Acta Crystallogr. Sect. A* **1995**, *51*, 33–38; e) G. P. van der Sluis, A. L. Spek, *Acta Crystallogr. Sect. A* **1990**, *46*, 3, 194–201.
[28] I. J. Bruno, J. C. Cole, P. R. Edgington, M. K. Kessler, C. F. Macrae, P. McCabe, J. Pearson, R. Taylor, *Acta Crystallogr. Sect. B* **2002**, *58*, 389–397.

Received: September 29, 2005
Revised: December 5, 2005
Published online: March 28, 2006

